

Indirect dark matter search with diffuse gamma rays from the Galactic Center with the Alpha Magnetic Spectrometer

A. Jacholkowska,^{1,*} G. Lamanna,² E. Nuss,¹ J. Bolmont,¹ C. Adloff,³ J. Alcaraz,⁴ R. Battiston,⁵ P. Brun,³ W. J. Burger,⁵ V. Choutko,⁶ G. Coignet,³ A. Falvard,¹ E. Fiandrini,⁵ L. Girard,³ C. Goy,³ K. Jedamzik,¹ R. Kossakowski,³ G. Moultaqa,¹ S. Natale,⁷ J. Pochon,³ M. Pohl,⁷ S. Rosier-Lees,³ M. Sapinski,^{1,†} I. Sevilla Noarbe,⁴ and J. P. Vialle³

¹Laboratoire de Physique Théorique et Astroparticules, UMR5207-UM2/IN2P3-CNRS,
Place Eugène Bataillon—CC70, 34095 Montpellier, France

²Centre de Physique des Particules de Marseille, UMR/IN2P3-CNRS, 163 avenue de Luminy—Case 902, 13288 Marseille, France

³Laboratoire d'Annecy-le-Vieux de Physique des Particules, LAPP/IN2P3-CNRS et Université de Savoie,
F-74941 Annecy-le-Vieux, France

⁴Centro de Investigaciones Energéticas, Medioambientales y Tecnológicas, CIEMAT, E-28040 Madrid, Spain

⁵University and Sezione INFN of Perugia, Italy

⁶Laboratory for Nuclear Science, MIT, 77 Massachusetts Avenue, Cambridge, Massachusetts 02171-9131, USA

⁷DPNC, University of Geneva, 24, Quai Ernest-Ansermet, 1211, Geneva 4, Switzerland

(Received 1 February 2006; published 18 July 2006)

The detection of nonbaryonic dark matter through its gamma-ray annihilation in the center of our galaxy has been studied. The gamma fluxes according to different models have been simulated and compared to those expected to be observed with the Alpha Magnetic Spectrometer (AMS), during a long-term mission on board of the international space station. Under the assumption that the dark matter is composed of the lightest, stable supersymmetric particle, the neutralino, the results of the simulations in the framework of minimal supergravity models, show that with a cuspy dark matter halo profile or a clumpy halo, the annihilation gamma-ray signal would be detected by AMS. More optimistic perspectives are obtained with the anomaly mediated supersymmetry breaking (AMSB) model. The latter leads also to a cosmologically important ${}^2\text{Li}$ abundance. Finally, the discovery potential for the massive Kaluza-Klein dark matter candidates has been evaluated and their detection looks feasible.

DOI: [10.1103/PhysRevD.74.023518](https://doi.org/10.1103/PhysRevD.74.023518)

PACS numbers: 95.35.+d

I. INTRODUCTION

The nature of dark matter is one of the outstanding questions and challenges in cosmology. The existence of cosmological dark matter is required by a multitude of observations and arguments, such as the excessive peculiar velocities of galaxies within clusters of galaxies, or the observations of gravitational arcs indicating much deeper gravitational potentials within clusters than those inferred by the presence of the luminous matter [1,2]. On the galactic scale, extensive dark matter halos are required to explain the observed rotation curves in spiral galaxies, or the velocity dispersion in elliptical galaxies [3,4]. Furthermore, big bang nucleosynthesis predicts a fractional contribution of baryons to the critical density, Ω_b , significantly smaller than the total Ω_m in form of clumpy matter. The Wilkinson Microwave Anisotropy Probe (WMAP) has provided the most detailed measurements of the cosmic microwave background (CMB) anisotropies [5]. In the framework of the standard cosmological model, WMAP quotes a total matter density of $\Omega_m = 0.27 \pm 0.04$ and a baryon density of $\Omega_b = 0.044 \pm 0.004$, which confirms that most of the matter is nonbaryonic, in agreement

with the results obtained from primordial nucleosynthesis studies.

Various nonbaryonic dark matter candidates require physics beyond the standard model of particle physics (for a recent review see e.g. [6]). N -body simulations of structure formation [7] suggest a nonrelativistic, weakly interacting massive particle (WIMP) as a dark matter component, thus favoring the cold dark matter scenario [8,9]. The WMAP measurement of the density of the nonbaryonic dark matter provides constraints in the range of $0.095 < \Omega_{\text{CDM}} h^2 < 0.129$, at the 2σ level.

Supersymmetric theories offer an excellent WIMP candidate, which satisfies the CDM paradigm and the constraints on Ω_{CDM} , namely, the neutralino (χ_1^0) of the minimal supersymmetric standard model (MSSM), assumed to be the lightest supersymmetric particle (LSP) and stable due to R -parity conservation [10]. At present, lower limits on the LSP neutralino mass in the MSSM are about 50 GeV from LEP experiments (although the mass may be significantly smaller depending on the assumptions relative to gaugino mass universality). Less conventional scenarios than the neutralino within the minimal supergravity (mSUGRA) context have been proposed [11]:

- (i) In the anomaly mediated supersymmetry breaking (AMSB) scenario [12,13] the neutralino LSP is predominantly a W -ino [the supersymmetric partner of the electrically neutral component of the $SU(2)_L$

*E-mail address: Agnieszka.Jacholkowska@cern.ch

†On leave from Henryk Niewodniczanski Institute of Nuclear Physics in Cracow

gauge bosons]. Endowed with a relatively large annihilation cross section this particle may constitute the bulk of the dark matter when subsequently to its thermal freeze-out, it is further generated non-thermally (e.g. via Q -ball evaporation or gravitino decay). By virtue of its large annihilation cross section the W -ino may lead to possibly large gamma fluxes [14].

- (ii) In extra-dimension models, ultimately motivated by string theories, it has been argued [15] that the lightest Kaluza-Klein excitation can provide under certain conditions, a very good CDM candidate. In the present paper we will restrict ourselves to the possibility of low scale extra-dimensions as an extension of the nonsupersymmetric standard model [16] with a perfectly viable dark matter Kaluza-Klein particle [17].

In this paper, we present the predicted γ -ray fluxes from the Galactic center from neutralino annihilations in the frame of mSUGRA and AMSB models, as well as from Kaluza-Klein dark matter annihilations. The predicted fluxes are used to assess, for the different scenarios, the discovery potential for nonbaryonic dark matter provided by a three-year observation of the diffuse γ -ray differential spectrum by the AMS on the ISS.

II. MODEL DESCRIPTIONS AND SIMULATIONS

The limited knowledge of dark matter structure and the density profile near the Galactic center represent the principal astrophysical uncertainties when evaluating the discovery potential of the dark matter through indirect detection. On the other hand, the predicted γ -ray fluxes depend on the assumptions made within the framework of the particle physics models associated with the different dark matter candidates.

A. Dark matter halo parametrization

One may parameterize the mass density profile of our Galaxy by the following equation:

$$\rho_\chi(r) = \rho_0 \left(\frac{R_0}{r} \right)^\gamma \left\{ \frac{R_0^\alpha + a^\alpha}{r^\alpha + a^\alpha} \right\}^\epsilon, \quad (1)$$

assuming a simple spherical Galactic halo. An isothermal profile with core radius a corresponds to $\gamma = 0$, $\alpha = 2$ and $\epsilon = 1$ as proposed by [18]. A Navarro, Frenk, and White (NFW) profile [19] is obtained with $\gamma = 1$, $\alpha = 1$, and $\epsilon = 2$, whereas Moore's distribution [20] is recovered if $\gamma = \epsilon = 3/2$ and $\alpha = 1$. Only the NFW and Moore models are considered in this study. The two models predict large values of the neutralino density in the Galactic center (GC).

The parameters of the halo modeling are:

- (i) R_0 —distance from Earth to GC,
- (ii) ρ_0 —halo density at R_0 ,

- (iii) a —the core radius—for $r < a$ the halo density is constant and equal to $\rho(a)$ in case of the isothermal parametrization.

As shown in [21], ρ_0 and a cannot be chosen arbitrarily. The total mass of the Galaxy restricts the (ρ_0, a) parameter space. For the NFW-*Standard* model the generic parameter values are: $R_0 = 8.0$ kpc, $\rho_0 = 0.3$ GeV/cm³, $a = 20$ kpc. Another possible combinations of (ρ_0, a) parameters allow, given the uncertainties: $R_0 = 8.5$ kpc, $\rho_0 = 0.4$ GeV/cm³, $a = 4$ kpc (NFW-*cuspy*). The two configurations were considered. The values for the Moore profile have been chosen as follows: $R_0 = 8.0$ kpc, $\rho_0 = 0.3$ GeV/cm³, $a = 28$ kpc.

The WIMPs located around the Galactic center should annihilate and produce high-energy photons. The corresponding photon flux near the Earth, Φ_γ —per unit time, surface, and solid angle—may be expressed as

$$\Phi_\gamma = \frac{1}{4\pi} \frac{\langle \sigma v \rangle N_\gamma}{2m_{\text{wimp}}^2} \int_{\text{los}} \rho_{\text{wimp}}^2(r) ds. \quad (2)$$

In Eq. (2), m_{wimp} is the mass of the WIMP-dark-matter candidate; $\langle \sigma v \rangle$ denotes the thermally averaged annihilation rate; $\rho_{\text{wimp}}(r)$ is the mass density of the dark matter and r is the distance from the Galactic center. The flux Φ_γ is proportional to the number of annihilations per unit time and volume, $\langle \sigma v \rangle \rho_{\text{wimp}}^2(r)/m_{\text{wimp}}^2$ and to the number of secondary photons per annihilation, N_γ . Finally to obtain the flux at the Earth it is necessary to integrate the WIMP density squared along the line-of-sight (los) connecting the observer to the Galactic center. The integral can be expressed in the form:

$$J(R) = 2 \int_0^{\sqrt{R_0^2 - R^2}} \rho^2(\sqrt{s^2 + R^2}) ds, \quad (3)$$

assuming a spherical halo with radial extension R_0 . The coordinate s extends along the line-of-sight. R is the radial distance from the center of the Galaxy for such a direction.

Because the density decreases steeply at large distances (see Eq. (1)), a radial cutoff R_c has been applied. It has been checked that our results are not sensitive to the value of R_c , which is set to 8.0 or 8.5 kpc depending on the chosen halo profile.

We integrate the function J over a solid angle around the Galactic center, subtended by the detector acceptance, e.g. a circular region with angular radius θ_{obs} :

$$\Sigma = 2\pi \int_0^{\theta_{\text{obs}}} J(R) \sin\theta d\theta, \quad (4)$$

where $R/R_0 = \tan\theta \simeq \theta$. Thus the resulting value for I_γ —flux of high-energy photons collected per unit of time and surface—can be written as:

$$I_\gamma = (3.98 \times 10^{-18} \text{ photons cm}^{-2} \text{ s}^{-1}) \left(\frac{\langle \sigma v \rangle N_\gamma}{10^{-29} \text{ cm}^3 \text{ s}^{-1}} \right) \times \left(\frac{1 \text{ TeV}}{m_\chi} \right)^2 \Sigma_{19}, \quad (5)$$

where Σ_{19} denotes Σ expressed in units of $10^{19} \text{ GeV}^2 \text{ cm}^{-5}$ and integrated over the AMS acceptance, $\Delta\Omega = 10^{-3} \text{ sr}$. We have integrated the relation (4) as a function of galactic halo profiles leading to the following results:

- (i) For a NFW-*standard* profile: $\Sigma_{19} = 2.7 \cdot 10^2$, thus $\tilde{J}(0)(\Delta\Omega) = 1.2 \cdot 10^3$
- (ii) For a NFW-*cuspy* profile: $\Sigma_{19} = 117.7 \cdot 10^2$, thus $\tilde{J}(0)(\Delta\Omega) = 50.0 \cdot 10^3$
- (iii) For a Moore profile: $\Sigma_{19} = 336.7 \cdot 10^2$, thus $\tilde{J}(0) \times (\Delta\Omega) = 142.9 \cdot 10^3$

where $\tilde{J}(0)(\Delta\Omega)$ corresponds to the notation used in [21]. For integration, we have defined an inner cutoff radius at $R_c = 10^{-5} \text{ pc}$ such that for $R > R_c$ the flux vanishes.

For completeness, two astrophysical factors may enhance the expected gamma fluxes from neutralino annihilations:

- (i) clumpiness of the dark matter halo as indicated by N -body simulations [7],
- (ii) the presence of a supermassive black hole (SBH) with a mass of $\sim 2.6 \times 10^6 M_\odot$ creating unstable conditions due to baryon infall by the adiabatic compression process, studied by [22,23]

The overall enhancement factor of the expected flux is estimated in [24] to be between 5 and 100, depending on the clumpiness of the galactic halo. The enhancement of the annihilation signal in presence of a spike in the dark matter halo is significant with respect to ordinary dark matter cusp, even in case of gravitational scattering of stars and the self-annihilating dark matter particles, as pointed by [22,25,26].

B. Models for WIMP candidates

In this section, we describe briefly the physics models associated with selected dark matter candidates, including the methodology and assumptions used to investigate the different hypotheses.

1. *mSUGRA parametrization*

The two supersymmetric scenarios considered belong to the class of models where supersymmetry (SUSY) breaking is effectively communicated to the visible sector via (super-)gravitational effects. We use the conventional *mSUGRA* scenario [11] with common values for the soft supersymmetry breaking scalar and gaugino masses and trilinear couplings, $m_0, m_{1/2}, A_0$, taken as initial conditions at a given high energy universality scale. We require the three gauge couplings to take a common value at a uni-

fication scale M_{GUT} and, for simplicity, identify this scale with the universality scale of the soft SUSY parameters. With these initial conditions and with the value of $\tan\beta$ (the ratio of the two Higgs vacuum expectation values $\frac{\langle H_u^0 \rangle}{\langle H_d^0 \rangle}$) defined at the electroweak scale, the relevant low energy quantities are obtained through the running of the parameters from M_{GUT} down to a scale of the order of the electroweak scale. Electroweak symmetry breaking is then required at that scale with the correct Z boson physical mass, thus fixing the supersymmetric μ parameter (up to a sign) and its soft supersymmetry breaking counterpart.

The flux predictions are obtained by use of computational tools which allow to scan over various SUSY parameters. This is achieved through an interface of the two codes, *DarkSUSY* [27] and *SUSPECT* [28], which we dub hereafter *DSS* (*DarkSUSY-SUSPECT*). Significant features of particle physics and cosmology are thus combined in our approach, taking into account various phenomenological constraints (consistency of the top, bottom and τ masses, present experimental limits on the superpartner and Higgs masses, limits from $b \rightarrow s\gamma$, no charged LSP, ..., relic density constraints), some of which are implemented in *SUSPECT* and others in *DarkSUSY*. We have checked in the *mSUGRA* framework the compatibility of the results obtained with the *DSS* software package and the *ISASUGRA* interface provided with *DarkSUSY*.

2. *Anomaly mediated supersymmetry breaking parametrization*

The anomaly mediated supersymmetry breaking (AMSB) is a gravity-mediated mechanism where the SUSY breaking is communicated to the observable sector by the super-Weyl anomaly [12,13]. In particular, the masses of gauginos are generated at the one-loop level as in [29]:

$$M_i = b_i \left(\frac{\alpha_i}{4\pi} \right)^2 \langle M \rangle, \quad (6)$$

where α_i are the gauge coupling constants and b_i the associated β -function coefficients. M is the auxiliary field in the supergravity multiplet whose vacuum expectation value $\langle M \rangle$ is expected to be of the order of the gravitino mass $m_{3/2}$, the latter being generically in the range: $10 \text{ TeV} < m_{3/2} < 100 \text{ TeV}$.

In the minimal AMSB model, the sleptons suffer typically from a tachyonic problem. One way to fix this problem is to add a scalar mass parameter m_0^2 , accounting for a nonanomalous contribution to the soft SUSY breaking.

The most important message from the gaugino mass formula above is the hierarchy:

$$M1:M2:M3 = 2.8:1:8.3$$

as opposed to $M1:M2:M3 = 1:2:7$ which is expected for the gravity- or gauge-mediated models. This implies that

the lightest neutralino ($\tilde{\chi}_1^0$) and the lightest chargino ($\tilde{\chi}_1^\pm$) are almost pure W -inos and consequently mass-degenerate.

3. Kaluza-Klein dark matter

Models with compact extra dimensions predict several new states, the Kaluza-Klein (KK) excitations. In the case of universal extra dimensions (UED) [16], all standard model fields can propagate in the bulk, and their effective four-dimensional interactions with the KK states conserve a quantum number associated with the latter. The conservation of this KK number implies that the KK modes cannot decay exclusively into standard model particles; the lightest KK mode (LKP) will thus be stable [16,30]. Moreover, the LKP, when electrically neutral and with no baryonic charge, provides a viable dark matter candidate [17]. The mass of the LKP dark matter particle, like all other states of the KK tower, is inversely proportional to the compactification radius R . Accelerator electroweak measurements constrain rather weakly the UED scenario, since in this scenario the observables are sensitive only to the virtual effects of the KK modes. The lower mass bound leads to $R^{-1} \geq 280$ GeV [16]. The most promising LKP dark matter candidate is associated with the first level of KK modes of the hypercharge gauge boson $B^{(1)}$. In our calculation we consider the relic density of $B^{(1)}$ of [17] leading to a $B^{(1)}$ lower bound mass bound constraint of 400 GeV.

III. AMS GAMMA DETECTION AND SENSITIVITY

A. The AMS-02 experiment

The main elements of AMS-02 detector [31] which are shown in Fig. 1 include: a superconducting magnet, a gaseous transition radiation detector (TRD), a silicon tracker (Tracker), time-of-flight hodoscopes (TOF), a

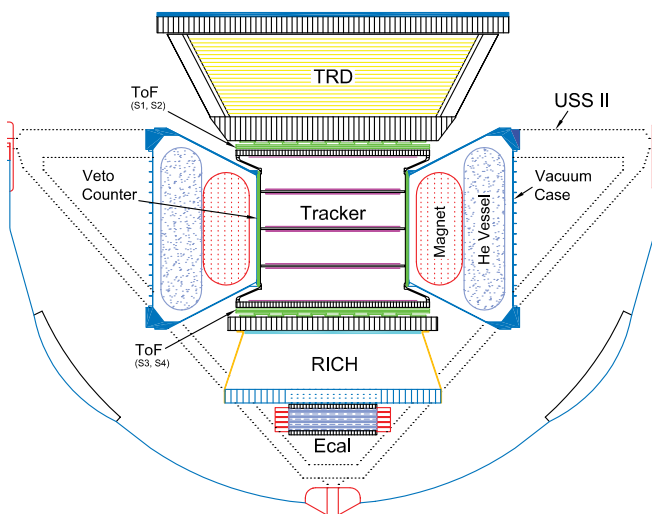


FIG. 1 (color online). Schematic view of the AMS-02 experiment which will operate on the International Space Station.

ring imaging Cerenkov detector (RICH), an electromagnetic calorimeter (ECAL) and anticoincidence Veto counters. The superconducting magnet has the shape of a cylindrical shell with the inner diameter of 1.2 m and length of 0.8 m; it provides a central dipole field of 0.8 Tesla. The eight layers of double-sided silicon tracker sensors are placed in planes transverse to the magnet axis. The silicon tracker measures the trajectory of relativistic singly charged particles with an accuracy of 10μ in the bending and 30μ in the nonbending coordinates. It provides also measurements of the particle energy loss which allows to distinguish the charge. The time-of-flight system (TOF) containing four detection layers, measures singly charged-particle transit times with an accuracy of 140 psec and also yields energy loss and coordinate measurements. The transition radiation detector (TRD) is situated on the top of the spectrometer and consists of 20 12 mm thick foam radiator arrays, interleaved by arrays of 6 mm diameter gas proportional tubes filled with a Xe/CO₂ mixture. The TRD provides an e^- /hadron separation better than 100 up to an energy of 200 GeV as well as precise charged-particle coordinate measurements. The RICH detector is installed below the last TOF plane and consists of a 3 cm thick aerogel radiator with a refraction index of 1.05, a mirror and pixel type matrix photo-tubes for the light detection measures of the velocity of the single charged particle with an accuracy better than a fraction of a percent. The ECAL detector is situated at the bottom of the AMS-02 setup. It is a three-dimensional ($65 \times 65 \times 17$ cm³ electromagnetic sampling calorimeter with total length of $16X_0$, consisting of 1 mm diameter scintillating fibers sandwiched between grooved lead plates.

B. Performance of photon detection

Cosmic γ -rays may be detected in AMS by two different methods. The *conversion mode* involves the reconstruction in the tracker of the e^+e^- pairs produced by γ conversions in the material upstream of the first layer of silicon sensors [32–34]. In the *single photon mode*, the γ -rays are detected in the electromagnetic calorimeter [35].

The performance of AMS-02 detector for γ -rays has been studied with the AMS simulation and reconstruction program based on GEANT [36]. The simulated performances have been validated using the AMS-01 data for the subdetectors present during the shuttle test flight [37] and the test beam data obtained with prototypes of the new or modified modules.

The Monte Carlo sample for the present study includes more than 10^9 reconstructed events including both cosmic γ -rays and charged-particle backgrounds over the relevant energy range. The latter in order of decreasing importance include protons, He and C nuclei and electrons. With a charged-particle background rejection of $O(10^4)$ to $O(10^5)$, we obtain a background-to-signal ratio of the order of a few

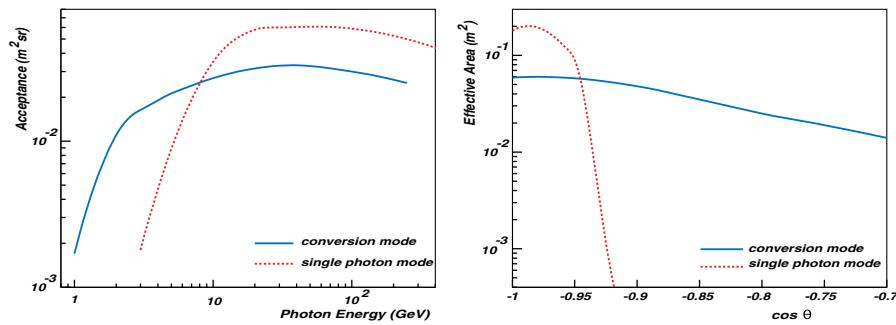


FIG. 2 (color online). AMS acceptance as a function of γ -ray energy for the two detection modes (top panel). The effective areas versus zenith angle at 50 GeV γ -ray energy (bottom panel).

percent. The principal background at this level is due to the galactic diffuse γ -ray emission.

1. The conversion mode

The event signature for this mode are two reconstructed tracks in the Tracker originating from a vertex located upstream of the first silicon layer of the tracker.¹

The incident γ -ray energy and direction were determined by adding the reconstructed momenta components of the e^\pm pair, evaluated at the entrance of the AMS-02 detector.

The main source of background are p and e^- which interact in the AMS detector, producing secondaries, mainly delta rays, which result in double-track events associated with a common origin at the interaction point.

The conversion of the secondary photons produced in the vicinity of the AMS, i.e. in the ISS body and solar panels, was found to be negligible in comparison to the expected γ -ray fluxes.

The following criteria are applied to reject background events:

- (i) Identify events with interactions;
- (ii) Identify charged particles entering the TRD from the top and fire all the tubes along its reconstructed trajectory.
- (iii) Identify reconstructed large invariant mass events.
- (iv) Identify particles entering the fiducial volume of the AMS through the side of the TRD.

A preliminary rejection factor of 5×10^4 was obtained for each different cosmic ray species (e^- and p), after all selection cuts have been applied.

2. The single photon mode

The event signature for this mode is the presence of electromagnetic-type energy deposition in the ECAL, while almost nothing is found in the other AMS subdetectors.

¹The material in front of the first silicon tracker plane, consists of the TRD, the first two layers of TOF scintillators, and mechanical supports, represents $\approx 0.23X_0$.

The identified backgrounds contributing to the cosmic γ -ray signal are events with charged particles² either passing undetected in the gaps of the AMS active tracking volume or entering the ECAL from the side.

The following criteria are applied to reject the background events:

- (i) Identify p , He by analyzing the 3-dimensional shower development in ECAL;
- (ii) Identify charged particles by requiring the trajectory direction of the reconstructed ECAL shower passes inside the AMS sensitive volume and reject these events.

The rejection factors for different cosmic ray species after all cuts have been applied are : $>6 \times 10^4$ for e^\pm , $(2.5 \pm 1) \times 10^6$ for p and $>1.7 \times 10^6$ for He nuclei.

3. Acceptances and resolutions

The simulations are used to parameterize the AMS performance for γ detection in terms of acceptance, effective area, angular and energy resolutions, and background rejection. Figure 2 shows the acceptance and effective area for the two detection modes. The corresponding energy and angular resolutions are shown in Fig. 3.³

The parameterized performance is used to establish the AMS-02 sensitivity for the different scenarios in which high-energy γ -rays are produced by the annihilation of dark matter near the Galactic center. In a first approximation, we consider a γ -ray source located at galactic longitude $l = 0$ and galactic latitude $b = 0$.

C. The sensitivity to the gamma flux and confidence level determination

We have developed a ROOT-based [39] simulation program, the AMS- γ fast simulator (AMSFS) [40], in order to investigate the AMS capability to localize nonisotropic radiation, either pointlike or diffuse. Here we describe the computational approach implemented in the simulator.

²mostly e^- , p and He nuclei

³We have chosen a conservative estimate of the single photon mode acceptance; a second study reports a 50% higher acceptance [38].

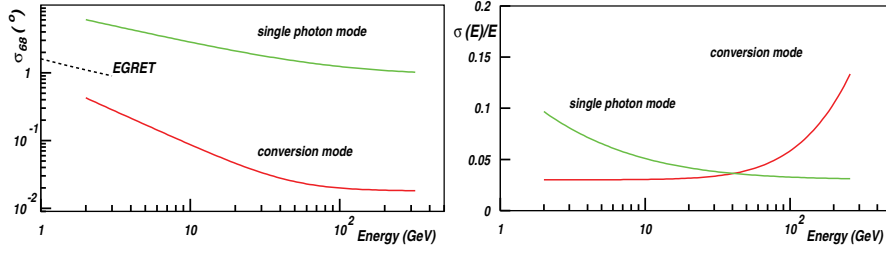


FIG. 3 (color online). The 68% containment angular resolution for both complementary detection modes as a function of energy (top panel). Energy resolutions as a function of original γ -ray energy (bottom panel).

We define the detector's γ -ray source sensitivity as the minimum flux required to achieve a specified level of detection significance. The significance S of a detection is given by:

$$S(E_\gamma > E_t) \sim \frac{N_\gamma^{\text{obs}}(E_\gamma > E_t)}{\sqrt{B(E_\gamma > E_t)}}, \quad (7)$$

where $N_\gamma^{\text{obs}}(E_\gamma > E_t)$ and $B(E_\gamma > E_t)$ are, respectively, the total number of detected photons from the source and the number of background photons falling within the source area above an energy threshold E_t . N_γ^{obs} and B are functions of the effective detection area $A(E)$ of the instrument, the angular resolution expressed in terms of the solid angle $\Omega(E)$, the observation time T_{obs} and the differential spectra:

$$N_\gamma^{\text{obs}}(E_\gamma > E_t) = \int_{E_t}^{\infty} \int_{\Omega} \frac{dN_\gamma}{dEd\Omega} A(E) T_{\text{obs}} d\Omega(E) dE, \quad (8)$$

and

$$B(E_\gamma > E_t) = \int_{E_t}^{\infty} \int_{\Omega} \frac{dB}{dEd\Omega} A(E) T_{\text{obs}} d\Omega(E) dE. \quad (9)$$

In order to establish the significance level of the observation, we require a minimum of three detected gamma events.

We use the analytical expressions resulting from the best fit to the curves shown in Figs. 2 and 3 for the energy dependence of the acceptance, the angular and energy resolutions. The solid angle over which the background is integrated for a given source is $\Omega(E) = \pi \sigma_{68}^2(E)$, where σ_{68} is the detector angular resolution defined within which 68% of the source photons fall.

The calculation of the Galactic center observation time T_{obs} is based on a 3-year mission on the international space station (ISS) [41]. The AMS observation time is not uniformly distributed over the celestial sphere since the ISS is in a 51.6° orbit, and the detector is fixed rigidly to the ISS. Taking into account the precession of the orbital plane of the station about the Earth's pole, a full sky coverage is obtained about 5.3 times per year. The *exposure* (effective area \times the observation time) varies with the

photon energy due to the energy dependence the effective area, and the position in the sky, due to the orbit precession.

The dependence of the effective area on the inclination of the photon direction (θ), the time dT_{obs} spent by the detector viewing the Galactic center within a specific viewing inclination $d\theta$, has been calculated and then integrated over the field-of-view (θ range up to 42° for the conversion mode and 22° for the single photon mode) and convoluted with the corresponding effective area: $A(E, d\theta) \times dT_{\text{obs}}$. The time intervals when ISS orbits over the South Atlantic anomaly region are excluded.

The source spectrum $dN_\gamma/dEd\Omega$ in Eq. (8) corresponds to the photon differential spectrum of the dark matter annihilation calculation incorporating the halo profile model and the choice of the particle physics parameters, including the mass of the WIMP candidate. The background flux $dB/dEd\Omega$ corresponds to the isotropic extra-galactic γ -ray background radiation and the galactic diffuse radiation (the latter is due mainly to the decay of π^0 s produced by interactions of the cosmic rays with the interstellar medium). The extra-galactic component has been measured by EGRET to be [42]:

$$\frac{dB_{\text{extragal.}}}{dEd\Omega} = \Phi_0 \times \left(\frac{E}{k_0}\right)^\epsilon \text{ (cm}^2 \text{ sr GeV)}^{-1}, \quad (10)$$

where $\Phi_0 = (7.32 \pm 0.34) \times 10^{-6} \text{ (cm}^2 \text{ sr GeV)}^{-1}$, $k_0 = 0.451 \text{ GeV}$ and $\epsilon = -2.10 \pm 0.03$.

The galactic diffuse flux is enhanced toward the galactic center and the galactic disk as measured by EGRET. In our calculation we use the parametrization of the differential flux provided in [21]:

$$\frac{dB_{\text{gal.}}}{dEd\Omega} = \Gamma_0 \times \left(\frac{E}{r_0}\right)^\alpha \text{ (cm}^2 \text{ sr GeV)}^{-1}, \quad (11)$$

where $\Gamma_0 = 8.6 \times 10^{-5} \text{ (cm}^2 \text{ sr GeV)}^{-1}$, $r_0 = 1 \text{ GeV}$ and $\alpha = -2.7$.

Finally, the Galactic center point sensitivity has to take into account the profile of the energy spectrum of the photons produced as a function of the neutralino mass m_χ . For this purpose we define the following function:

$$\Lambda(m_\chi) = \frac{\int_{E_t}^{\infty} \frac{d\Phi}{dE} A(E) dE}{\int_{E_t}^{\infty} \frac{d\Phi}{dE} dE}. \quad (12)$$

$\Lambda(m_\chi)$ includes the weight of the detector acceptance $A(E)$ on the total rate of photons expected to be detected for a given differential flux

$$\frac{d\Phi}{dE} = \frac{1}{4\pi} \frac{dN_\gamma}{dE} \frac{\langle\sigma v\rangle}{2m_\chi^2} \Sigma_{19}. \quad (13)$$

Therefore we can rewrite the function Λ as

$$\Lambda(m_\chi) = \frac{\int_{E_t}^{\infty} \frac{dN_\gamma}{dE} A(E) dE}{\int_{E_t}^{\infty} \frac{dN_\gamma}{dE} dE}, \quad (14)$$

where

$$\int_{E_t}^{\infty} \frac{dN_\gamma}{dE} dE = N_\gamma(E_\gamma \geq E_t) \quad (15)$$

is the total number of continuum γ -rays above energy E_t mainly due to the decay of π^0 mesons produced in jets from neutralino annihilation. For the computation of N_γ we have considered the parametrization from Ref. [43], after checking its compatibility with PYTHIA parametrization included in DSS as explained in the caption of Fig. 4:

$$N_\gamma(E_\gamma \geq E_t) = \frac{5}{6} \left(\frac{E_t}{m_\chi}\right)^{3/2} - \frac{10}{3} \frac{E_t}{m_\chi} + 5 \left(\frac{E_t}{m_\chi}\right)^{1/2} + \frac{5}{6} \left(\frac{E_t}{m_\chi}\right)^{-1/2} - \frac{10}{3}. \quad (16)$$

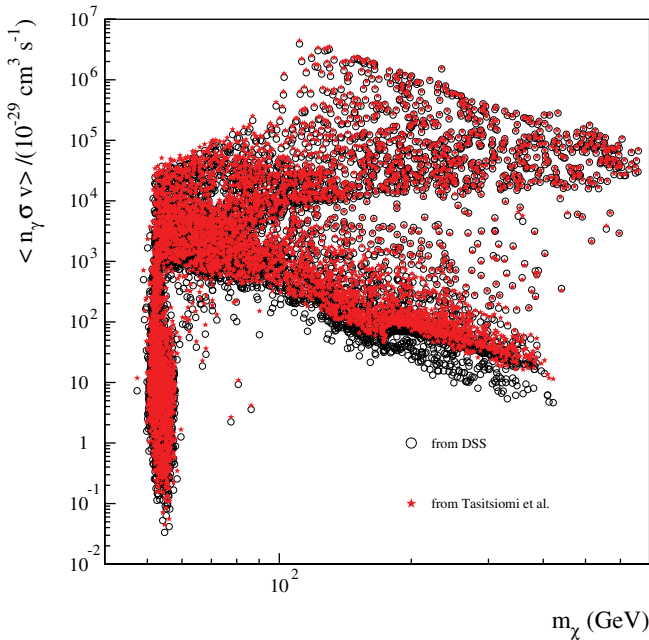


FIG. 4 (color online). The $\langle N_\gamma \sigma v \rangle$ as a function of m_χ with standard set of parameters as compared with parametrization [43]. A threshold $E_t = 1$ GeV has been assumed. A normalization factor of 2.4 was applied to obtain compatibility between the two calculations. This factor is used in our calculations.

The differential continuum spectrum, assuming $N_\gamma(E_t = m_\chi) = 0$, is:

$$\frac{dN_\gamma}{dE} = \frac{1}{m_\chi} \left(\frac{10}{3} + \frac{5}{12} \left(\frac{E}{m_\chi}\right)^{-3/2} - \frac{5}{4} \left(\frac{E}{m_\chi}\right)^{1/2} - \frac{5}{2} \left(\frac{E}{m_\chi}\right)^{-1/2} \right). \quad (17)$$

With formulas (16) and (17) we can compute the function $\Lambda(m_\chi)$ for a given value of the neutralino mass m_χ :

$$\Lambda(m_\chi) = \frac{1}{N_\gamma} \int_{E_t}^{\infty} \frac{dN_\gamma}{dE} A(E) dE \quad (18)$$

and obtain the corresponding confidence level.

The total number of photons detected by AMS is defined as

$$N_\gamma^{\text{obs}}(E_\gamma > E_t) = T_{\text{obs}} \int_{E_t}^{\infty} \frac{d\Phi}{dE} A(E) dE. \quad (19)$$

or, using the $\Lambda(m_\chi)$ function

$$N_\gamma^{\text{obs}}(E_\gamma > E_t) = T_{\text{obs}} \Lambda(m_\chi) \int_{E_t}^{\infty} \frac{d\Phi}{dE} dE. \quad (20)$$

According to the detectability criterion defined in Eq. (7), the minimum detectable flux F_{min} , which corresponds to a significance $S(E_\gamma > E_t) = 3$, is derived by requiring $N_\gamma^{\text{obs}} = 3\sqrt{B}$. The definition of:

$$\Phi_{95} = \int_{E_t}^{\infty} \frac{d\Phi_{\text{min}}}{dE} dE = \frac{3\sqrt{B(E_\gamma > E_t)}}{\Lambda(m_\chi) T_{\text{obs}}} \quad (21)$$

leads to conservative 95%–99% Confidence Level values.

IV. RESULTS

A. mSUGRA and benchmark point simulations

The DSS program provides values of the γ -ray fluxes for the SUSY benchmark models [44,45] and the so-called “wild scan” configurations of the mSUGRA parameters.

The SUSY benchmark models have been proposed to provide a common way of comparing the SUSY discovery potential of the future accelerators such as LHC or linear colliders. The 13 SUSY scenarios correspond to different configurations of the five mSUGRA parameters with the trilinear coupling parameter A_0 set to 0. The models fulfill the conditions imposed by LEP measurements, the $g_\mu - 2$ result, and the relic density constraint of $0.094 < \Omega_\chi h^2 < 0.129$.

To derive the gamma-ray fluxes for some of these benchmark models we use our current MC simulation programs: DSS, which was described previously. In particular the value of $\Omega_\chi h^2$ is calculated in the DarkSUSY part, while the simultaneous use of the SUSPECT and DarkSUSY

TABLE I. The lightest neutralino mass m_χ , the mSUGRA parameters m_0 , $\tan\beta$, the relic neutralino densities, i.e. $\Omega_\chi h^2$ and the values $\langle N_\gamma \sigma v \rangle$ as described in the text in units of $10^{-29} \text{ cm}^3 \text{ s}^{-1}$; (masses are in GeV and the stars indicate values from [46]).

model	B	G	I	K	L
M_χ	98.3	153.6	143.0	571.5	187.2
m_0	59	116	178	999	299
$\tan\beta$	10.0	20.0	35.0	38.2	47.0
$\Omega_\chi h^2$	0.12	0.12	0.12	0.11	0.10
$\Omega_\chi h^{2*}$	0.12	0.13	0.13	0.09	0.10
$\langle n_\gamma \sigma v \rangle$	1013	1283	8380	29344	33438
$\langle n_\gamma \sigma v \rangle^*$	782	1032	6303	70903	18739

package allows to perform Renormalization Group Equations evolution from the GUT scale to EWSB scale.

Table I presents values of the lightest neutralino mass m_χ , the mSUGRA parameters m_0 , $\tan\beta$, the neutralino relic density $\Omega_\chi h^2$ and the values $\langle N_\gamma \sigma v \rangle$ as described in Sec. III.

The corresponding values of neutralino mass, $\tan\beta$ and m_0 are also quoted. A fine-tuning procedure has been applied as in [44] (to fulfill the relic density constraints). The N_γ were obtained with fast simulation by the convolution of the differential γ -ray fluxes with angular and energy resolution, and applying the acceptance factors of the tracker (TR) and calorimeter (ECAL).

The choice of the benchmark model sample was guided by the requirement of meaningful flux values. These values are low, however, in more favorable astrophysical scenarios, the expected N_γ are enhanced by substantial factors varying from 40 in case of the most cuspy NFW halo profile or about a hundred in case of a Moore profile.

The results in Table I are also compared to those in [46], where a different mSUGRA Monte Carlo was used. Good agreement was found between the results of the two cal-

TABLE II. The expected number of photons detected in 3 years for different benchmark models and various dark matter halo profiles. Since the benchmark model flux values are low in the scanned (Φ_γ, m_χ) plane, a 3 GeV energy cut threshold has been applied for signal and diffuse gamma background calculations. The sensitivities (N_σ = number of standard deviations above diffuse gamma emission) have been calculated only for photons detected in the tracker assuming 3.0 background photons. In the ECAL detector, we expect 196.0 photons for the galactic diffuse gamma emission.

model	B	G	I	K	L
$N_{\gamma\text{std}}^{\text{NFW}}$	0.22	0.14	0.94	0.35	2.48
$N_{\gamma\text{cuspy}}^{\text{NFW}}$	9.2	6.0	40.8	15.2	107.8
$N_{\gamma}^{\text{Moore}}$	26.4	17.1	117.3	43.7	309.9
$S/B_{\text{std}}^{\text{NFW}}$	0.04	0.03	0.18	0.06	0.45
$N_{\sigma\text{cuspy}}^{\text{NFW}}$	3.2	1.9	13.8	4.7	35.8
$N_{\sigma}^{\text{Moore}}$	8.9	5.7	39.6	13.5	102.8

culations. The observed differences for $\langle N_\gamma \sigma v \rangle$, which are at most $\sim 25\%$ between our results and those in [46], may be explained by more refined interfacing.

In Table II, N_γ detected by AMS during 3-year observation and the significance values for the benchmark models are presented for the NFW halo profile with the standard set of parameter, the most cuspy NFW profile and the Moore profile. The diffuse γ -ray background has been evaluated with the procedure described in Sec. III. The hadron contribution can be considered negligible for a pointlike source, as the proton suppression factors range between 10^{-5} and 10^{-6} . For the standard NFW profile, only the values of the signal-to-background ratio are given as the expected N_γ values are not significant.

B. Predictions from “wild scan” simulations

1. mSUGRA results

We have performed a “wild scan” in the mSUGRA parameter space. Six thousand models have been simulated in the region of $0.0 \leq \Omega_\chi h^2 \leq 0.129$. The values below the WMAP lower constraint on $\Omega_\chi h^2$ (0.094) belong to the additional nonthermal neutralino production scenarios.

The ranges of the mSUGRA parameters used in the simulation were:

$$\begin{aligned} \text{sign}(\mu) & \text{not constraint} \\ 50. & < m_0 < 3000. \\ 50. & < m_{1/2} < 1600. \\ 0.1 & < |A_0| < 2000. \\ 3. & < \tan(\beta) < 60. \end{aligned}$$

The results for the integrated gamma fluxes from the Galactic center as a function of the χ_1^0 mass, presented in Fig. 5, were obtained for a NFW-*standard* profile, and for a γ -ray energy threshold of $E_\gamma = 1$ GeV. Figure 6 shows the results for the more favorable NFW cuspy dark matter profile.

2. AMSB results

For the prediction of the gamma-ray flux in the AMSB framework, the scheme proposed by SUSPECT was used for the evolution of the AMSB parameters up to the EWSB, as for our mSUGRA simulations. Therefore we use the same DSS interface.

The constraints set on the four AMSB parameters (as described in [46]) were:

$$\begin{aligned} \text{sign}(\mu) & \text{not constraint} \\ 10^4 & < M_{3/2} < 10^6. \\ 10^3 & < a_0 < 15 \cdot 10^3 \\ 3. & < \tan(\beta) < 60. \end{aligned}$$

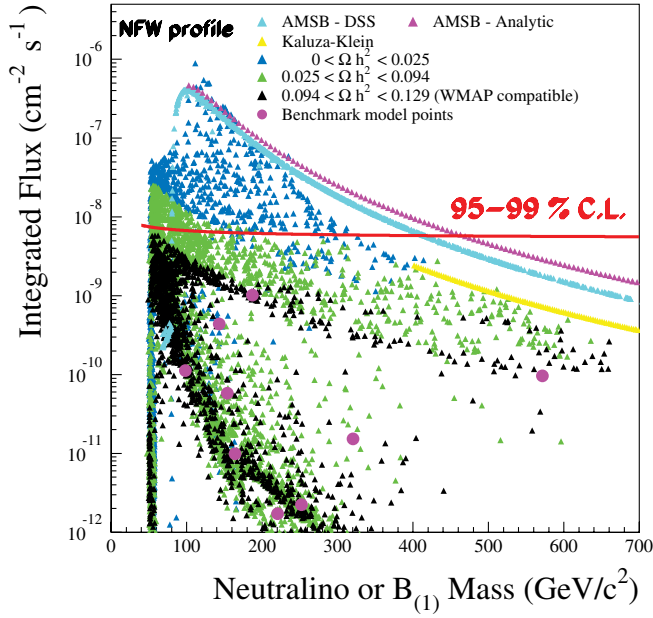


FIG. 5 (color online). The integrated γ flux from the Galactic center as a function of m_χ for the NFW halo profile parametrizations with the standard set of parameters. The considered models are the mSUGRA scheme, AMSB scenario and Kaluza-Klein universal extra-dimensions. The various selections were done by varying Ωh^2 cuts.

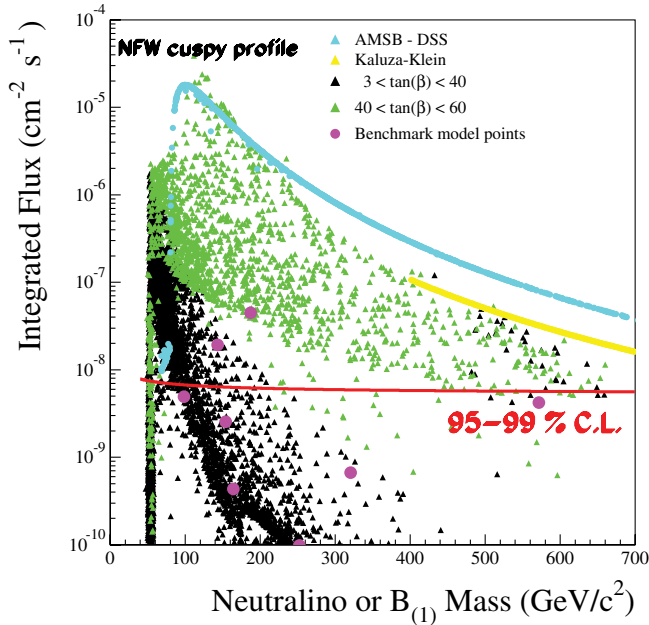


FIG. 6 (color online). The integrated γ flux from the Galactic center as a function of m_χ for a cuspy NFW dark matter halo profile as described in the text. The considered models are the mSUGRA scheme, AMSB scenario and Kaluza-Klein universal extra dimensions. The various selections were done by varying $\tan(\beta)$ cuts.

For completeness, we have checked that this approach was compatible with the analytical approximation as described below.

From Eq. (2) we get:

$$\Phi_\gamma(\Delta\Omega, E_\gamma > E_t) = 1.19 \cdot 10^{-14} N_\gamma \left(\frac{\langle\sigma\beta\rangle}{pb} \right) \times \left(\frac{1 \text{ TeV}}{m_\chi} \right)^2 \Sigma_{19} \text{ cm}^{-2} \text{ s}^{-1}, \quad (22)$$

and under the hypothesis of a pure W -ino LSP, the pair annihilation proceeds by exchange of a charged W -ino. The neutral W -ino, here assumed to be the WIMP-LSP, can annihilate into a W -boson pair ($\tilde{W}^0 \tilde{W}^0 \rightarrow W^+ W^-$). We have considered the results of [29] for the parametrization of the corresponding annihilation cross section, in the nonrelativistic limit:

$$\langle\sigma\beta\rangle = 9.77 \left(\frac{1 \text{ TeV}}{m_\chi} \right)^2 \frac{(1 - x_W)^{3/2}}{(2 - x_W)^2} pb, \quad (23)$$

where $x_W = m_W^2/m_\chi^2$.

Thus the equation for the integral flux of photons from W -ino LSP annihilation becomes:

$$\Phi_\gamma(\Delta\Omega, E_\gamma > E_t) = 1.16 \cdot 10^{-13} N_\gamma \frac{(1 - x_W)^{3/2}}{(2 - x_W)^2} \times \left(\frac{\text{TeV}}{m_\chi} \right)^4 \Sigma_{19} \text{ cm}^{-2} \text{ s}^{-1}, \quad (24)$$

where we have used Eq. (17) for the N_γ value with the scaling factor as described in the caption of Fig. 4.

C. Kaluza-Klein results

The main annihilation channels of LKP into standard model particles are charged lepton pairs for about 59% and quark pairs for about 35% [47]. In our case, the calculation of secondary gamma-ray yield were based on the formulas of $\sigma v(B^{(1)} B^{(1)} \rightarrow f \bar{f})$ [17]. The contribution of gamma rays produced from channels with leptons [48] has been neglected, thus providing more conservative results for the gamma fluxes at high energies. As in our previous calculations and following [47] we have used Eq. (25) with again the N_γ value from Eq. (17). To obtain the flux for a given halo profile, we have used the corresponding value of Σ_{19} given in the paragraph 2.1, thus resulting in:

$$\Phi_\gamma(\Delta\Omega, E_\gamma > E_t) = 7.2 \cdot 10^{-15} N_\gamma \left(\frac{1 \text{ TeV}}{m} \right)^4 \times \Sigma_{19} \text{ cm}^{-2} \text{ s}^{-1} \quad (25)$$

We checked that our results are compatible with [6]. The expected γ fluxes for the AMSB models and Kaluza-Klein models are also shown in Figs. 5 and 6.

D. Sensitivity for considered models

The 95% CL was obtained by varying, within the uncertainties, the diffuse γ background spectrum as measured by EGRET [49] in the Galactic center area, as described in Sec. III C. With a required minimum of 3 photons over 3σ of the diffuse gamma background and a 1 GeV energy threshold and 3 yr exposure time, the sensitivity to Galactic Center measurements is $(7.0 \pm 0.4)10^{-9} \text{ cm}^{-2} \text{ s}^{-1}$ with only a small residual dependence on m_χ . For both sets of astrophysical conditions, the predicted γ fluxes for the AMSB and Kaluza-Klein models are above the 95% CL for WIMP masses below 400 GeV. This indicates the potential of detection or exclusion of AMS-02 in the case of the less conventional SUSY scenario with nonthermal production of neutralinos, or other dark matter candidate proposed by the Kaluza-Klein extra-dimension theories.

It has been recently shown [50] that residual dark matter annihilation during the epoch of big bang nucleosynthesis may result in an efficient production of ${}^6\text{Li}$. In Fig. 7 we show the resulting ${}^6\text{Li}/\text{H}$ ratio in the dark matter models studied in this paper. The ${}^6\text{Li}/\text{H}$ yields have been calculated using the parametrizations given in Ref. [50]. The predicted abundances are compared to the value reported for the low-metallicity halo stars, such as HD84937, ${}^6\text{Li}/\text{H} \approx 8.47 \pm 3.10 \times 10^{-12}$ [51], (one of the first stars where a ${}^6\text{Li}$ detection had been claimed). It is seen that, even in a context of a standard NFW profile (Fig. 5), the observed ${}^6\text{Li}$ abundance is consistent with values produced

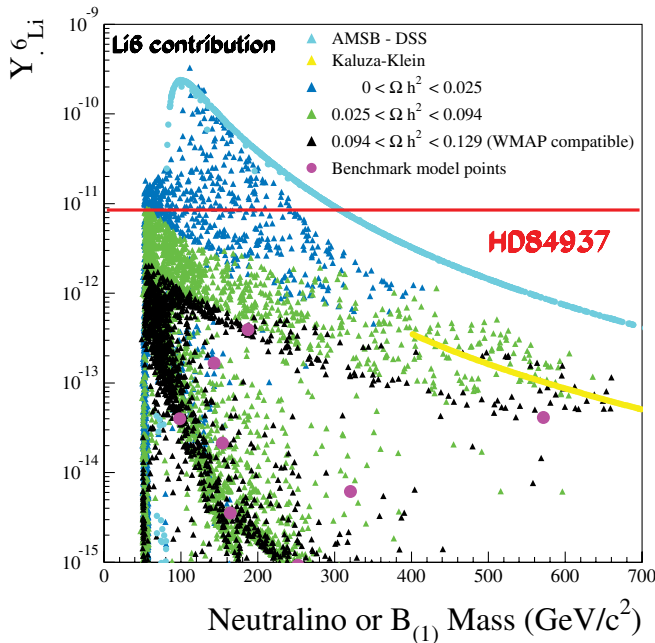


FIG. 7 (color online). The resulting ${}^6\text{Li}/\text{H}$ yield synthesized due to residual neutralino/Kaluza-Klein annihilation during the epoch of big bang nucleosynthesis for the same models as considered before. Also shown is the central value of the ${}^6\text{Li}/\text{H}$ as observed in the low-metallicity star HD84937.

with certain model configurations, in particular, in non-thermal scenarios for the AMSB model. Detections of ${}^6\text{Li}$ have been reported for ~ 10 other stars [52,53], with abundances comparable to HD84937. As this is far from what expected in cosmic ray scenarios which may synthesize ${}^6\text{Li}$, it is possible that the ${}^6\text{Li}$ abundance in low-metallicity stars is in fact an indirect signal of dark matter annihilation during big bang nucleosynthesis.

V. CONCLUSIONS

The DarkSUSY and SUSPECT programs were used to provide the γ -ray flux predictions from the Galactic center region, for the benchmark mSUGRA models, the AMSB scenario and Kaluza-Klein Universal Extra-dimensions models, in order to evaluate the discovery potential of AMS for nonbaryonic dark matter. Only models of mSUGRA scenario with large $\tan\beta$ yield measurable signals on a realistic time scale. This conclusion is confirmed in a second study with a “wild scan” mSUGRA simulations. Various aspects such as dependence of the results on heavy quark masses or CP -odd Higgs pole contributions may change the predictions [24]. The most significant signals correspond to the supersymmetric configurations with the neutralino mass $m_\chi \sim 100$ GeV.

The sensitivity of the AMS-02 detector for γ -ray fluxes from a pointlike source will allow to detect fluxes smaller by a factor of 2 to 3, compared to those measured by EGRET experiment in the GeV range, in the Galactic center region [49]. AMS mission will also extend these measurements to a poorly explored energy range around 10 GeV, important for the detection of a low mass neutralino. In the TeV range, the Galactic center was observed by ground-based Air Shower Cherenkov Telescopes (ACTs), which have detected several intensive astrophysical sources [54,55]. The signal from the central source, as observed by different ACT experiments, has been analyzed in the context of SUSY dark matter by [56]. More recently, the HESS Collaboration has published a discovery of a diffuse γ emission in the galactic plane in TeV range, nearby the SgrA* emitter, possibly produced by the hadronic interactions of the Galactic cosmic rays with a complex of molecular clouds [57]. These results indicate that the choice of the observed dark matter source is crucial, and the intense astrophysical environment may be an obstacle for an exotic signal detection. A more promising type of dark matter source could be a nearby Dwarf Spheroidal Galaxy such as DRACO, Sagittarius or Canis Major, presenting lower standard astrophysical backgrounds. These sources have been considered by several authors for the SUSY dark matter flux predictions [58,59], and their observation campaigns have been scheduled by ACT telescope experiments in the coming future.

In the frame of the present study with the Galactic center source, the 3 yr observation with AMS detector would provide 95% CL exclusion limits for several mSUGRA

models in the case of a favorable dark matter galactic halo configuration, such as the cuspy or very cuspy NFW profiles. Furthermore, if the halo is made of clumps with inner profiles of cuspy type, or if there is a strong accretion around the central black hole, the expected signal would increase by 2 orders of magnitude. For such cases, given the excellent energy resolution of the detector, the discovery of a dark matter annihilation signal would be possible. In particular, the nonthermal SUSY Breaking scenarios, as in case of the AMSB model, result in cosmologically significant ${}^6\text{Li}$ abundances, which, when confronted with

the results for ${}^6\text{Li}$ abundances in low-metallicity stars offer interesting perspectives for indirect dark matter searches and the detection of an annihilation signal by AMS. We conclude, that a survey of the Galactic center by AMS has the potential to contribute significantly to our understanding of dark matter.

ACKNOWLEDGMENTS

We thank all our colleagues from AMS for expressing their support and interest in this study.

-
- [1] N. Bahcall and X. Fan, *Astrophys. J.* **504**, 1 (1998).
 [2] N. Dalal and C. R. Keeton, *astro-ph/0312072*.
 [3] M. Azzaro, F. Prada, and C. M. Gutierrez, *astro-ph/0310487*.
 [4] D. Zaritsky *et al.*, *Astrophys. J. Suppl. Ser.* **478**, 39 (1997).
 [5] C. L. Bennett *et al.* *Astrophys. J. Suppl. Ser.* **148**, 1 (2003).
 [6] G. Bertone, D. Hooper, and J. Silk, *Phys. Rep.* **405**, 279 (2005).
 [7] J. R. Primack, *Proceedings of International School of Space Science 2001*, edited by Aldo Morselli, Frascati Physics Series (to be published).
 [8] G. Jungman, M. Kamionkowski, and K. Griest, *Phys. Rep.* **267**, 195 (1996).
 [9] L. Bergstrom, *Rep. Prog. Phys.* **63**, 793 (2000).
 [10] H. Goldberg, *Phys. Rev. Lett.* **50**, 1419 (1983); J. Ellis *et al.*, *Phys. Lett. B* **127**, 233 (1983).
 [11] R. Barbieri, S. Ferrara, and C. A. Savoy, *Phys. Lett. B* **119**, 343 (1982); A. H. Chamseddine, A. Arnowitt, and P. Nath, *Phys. Rev. Lett.* **49**, 970 (1982); L. J. Hall, J. Lykken, and S. Weinberg, *Phys. Rev. D* **27**, 2359 (1983); N. Ohta, *Prog. Theor. Phys.* **70**, 542 (1983).
 [12] L. Randall and R. Sundrum, *Nucl. Phys.* **B557**, 79 (1999).
 [13] G. Giudice *et al.*, *J. High Energy Phys.* **12** (1998) 027.
 [14] D. Hooper and L. Wang, *Phys. Rev. D* **69**, 035001 (2004).
 [15] E. W. Kolb and R. Slansky, *Phys. Lett. B* **135**, 378 (1984).
 [16] T. Appelquist, H. C. Cheng, and B. A. Dobrescu, *Phys. Rev. D* **64**, 035002 (2001).
 [17] G. Servant, and T. M. P. Tait, *Nucl. Phys.* **B650**, 391 (2003).
 [18] G. Gentile *et al.*, *Mon. Not. R. Astron. Soc.* **351**, 903 (2004).
 [19] J. F. Navarro, C. S. Frenk, and S. D. M. White, *Astrophys. J.* **462**, 563 (1996).
 [20] B. Moore *et al.*, *Phys. Rev. D* **64**, 063508 (2001).
 [21] L. Bergstrom, P. Ullio, and J. H. Buckley, *Astropart. Phys.* **9**, 137 (1998).
 [22] G. Bertone and D. Merritt, *Phys. Rev. D* **72**, 103502 (2005).
 [23] P. Gondolo and J. Silk, *Phys. Rev. Lett.* **83**, 1719 (1999).
 [24] A. Falvard *et al.*, *Astropart. Phys.* **20**, 467 (2004).
 [25] P. Ullio, H. S. Zhao, and M. Kamionkowski, *Phys. Rev. D* **64**, 043504 (2001).
 [26] J. Edsjo *et al.*, *J. Cosmol. Astropart. Phys.* **09** (2004) 004.
 [27] <http://www.physto.se/~edsjo/darksusy/>.
 [28] A. Djouadi, J.-L. Kneur, and G. Moutaka, *hep-ph/0211331*.
 [29] T. Moroi and L. Randall, *Nucl. Phys.* **B570**, 455 (2000).
 [30] T. G. Rizzo, *Phys. Rev. D* **64**, 095010 (2001); C. Macesanu, C. D. McMullen, and S. Nandi, *Phys. Rev. D* **66**, 015009 (2002); H. C. Cheng, K. T. Matchev, and M. Schmaltz, *Phys. Rev. D* **66**, 036005 (2002).
 [31] AMS Collaboration, *Nucl. Instrum. Methods*, (to be published).
 [32] R. Battiston *et al.*, *Astropart. Phys.* **13**, 51 (2000).
 [33] G. Lamanna, *Nucl. Phys. B, Proc. Suppl.* **113**, 177 (2002).
 [34] G. Lamanna, *AMS-Note 2003-03-03*.
 [35] V. Choutko, G. Lamanna, and A. Malinin, *Int. J. Mod. Phys. A* **17**, 1817 (2002).
 [36] S. Agostinelli *et al.* (Geant4 collaboration), *NIM A* **506**, 250 (2003).
 [37] M. Aguilar *et al.*, *Phys. Rep.* **366**, 331 (2002).
 [38] L. Girard, *Proceedings to Moriond—Astroparticle 2005 and references therein*.
 [39] <http://root.cern.ch>.
 [40] J. Bolmont, Ph.D. thesis, Univ. Montoellier II, 2005.
 [41] I. Sevilla Noarbe, *AMS-Note 2004-03-03*.
 [42] P. Sreekumar *et al.*, *Astrophys. J.* **494**, 523 (1998).
 [43] A. Tasitomi and A. V. Olinto, *Phys. Rev. D* **66**, 083006 (2002).
 [44] M. Battaglia *et al.*, *Eur. Phys. J. C* **24**, 311 (2002).
 [45] J. Ellis *et al.*, *Eur. Phys. J. C* **24**, 311 (2002).
 [46] P. Gondolo *et al.*, *J. Cosmol. Astropart. Phys.* **07** (2004) 008.
 [47] G. Bertone, G. Servant, and G. Sigl, *Phys. Rev. D* **68**, 044008 (2003).
 [48] L. Bergstrom, *et al.*, *Phys. Rev. Lett.* **94**, 131301 (2005).
 [49] S. D. Hunter *et al.*, *Astrophys. J.* **481**, 205 (1997).
 [50] K. Jedamzik, *Phys. Rev. D* **70**, 063524 (2004); **70**, 083510 (2004).
 [51] R. Cayrel *et al.*, *Astron. Astrophys.* **343**, 923 (1999).
 [52] P. E. Nissen *et al.*, *astro-ph/0004251*.
 [53] P. E. Nissen *et al.*, *Astron. Astrophys.* **348**, 211 (1999).
 [54] F. Aharonian *et al.* (HESS Collaboration), *Astron. Astrophys.* **425**, L13 (2004); L. Rolland and J. Hinton (HESS collaboration), *Proceedings of ICRC conference, Pune, India* (2005).

- [55] M. Mori (CANGAROO collaboration), Proceedings of 28th ICRC conference (2003), vol. 5. **439**, 695 (2006).
- [56] S. Profumo, Phys. Rev. D **72**, 103521 (2005).
- [57] F. Aharonian *et al.* (HESS collaboration), Nature (London) **439**, 695 (2006).
- [58] N. W. Evans, F. Ferrer, and S. Sarkar, Phys. Rev. D **69**, 123501 (2004).
- [59] D. Hooper *et al.*, Phys. Rev. Lett. **93**, 161302 (2004).